Strain-Induced Two-Dimensional Electron Gas in Selectively Doped Si/Si_xGe_{1-x} Superlattices

G. Abstreiter, H. Brugger, and T. Wolf
Physik-Department E 16, Technische Universität München, D-8046 Garching, Federal Republic of Germany

and

H. Jorke and H. J. Herzog
AEG-Telefunken, Forschungsinstitut, D-7900 Ulm, Federal Republic of Germany
(Received 2 April 1985)

We report the observation of two-dimensional electron systems and enhanced mobilities in $Si/Si_{0.5}Ge_{0.5}$ strained-layer multilayer structures. The built-in strain is measured by phonon Raman spectroscopy. The mobility enhancement depends strongly on the position of the doped region within the layers. The experimental results can be explained in a consistent way when carrier confinement in the Si layer is assumed. The importance of the built-in strain in lowering the conduction band in Si is emphasized.

PACS numbers: 73.40.Lq, 63.20.Dj, 72.20.My

In this communication we report on observations of the two-dimensional nature of electron gases and of mobility enhancement in selectively doped Si/Si_xGe_{1-x} strained-layer superlattices. This type of multilayer structures has received considerable attention during the past few years. In spite of the relatively large lattice mismatch of about 4% between Si and Ge, high-quality pseudomorphic growth of Si/Si_xGe_{1-x} multilayer structures has been achieved by molecular beam epitaxy (MBE).[1-4] The built-in strain in the layers has been investigated very effectively by Raman scattering experiments.[5] Recently, mobility enhancement of two-dimensional holes in selectively doped $Si/Si_{0.8}Ge_{0.2}$ heterostructures has been reported.[6] In those samples, holes are transferred in space from the acceptor states in the wider-gap material Si to the valence band of the $Si_{0.8}Ge_{0.2}$ alloy. There was no evidence for electron confinement in *n*-type samples. However, as shown recently, electron mobility enhancement can be achieved by selective Sb doping of Si/Si_xGe_{1-x} strained-layer superlattices.[7] The incorporation of the *n*-type dopant antimony was performed by a method denoted as secondary implantation. Details of this method are discussed elsewhere.[8]

In the present work we discuss various experimental aspects that demonstrate the two-dimensional nature of the carrier system, a strong low-temperature mobility enhancement, and the carrier confinement in Si rather than in the Si_xGe_{1-x} layers. To investigate the built-in strain, we used phonon Raman scattering. Enhanced transport properties were studied by low-temperature Hall measurements and Shubnikov–de Haas and cyclotron-resonance experiments. A new model for the conduction-band ordering is presented which emphasizes the importance of strain on band offsets.

The layer sequence is shown schematically as an inset in Fig. 1. A $Si_{0.75}Ge_{0.25}$ buffer layer of 200-m thickness is followed by a periodic sequence of $\simeq 6$-nm Si and 6-nm $Si_{0.5}Ge_{0.5}$. The total number of periods is ten. The buffer layer is incorporated in order to achieve a medium lattice spacing between that

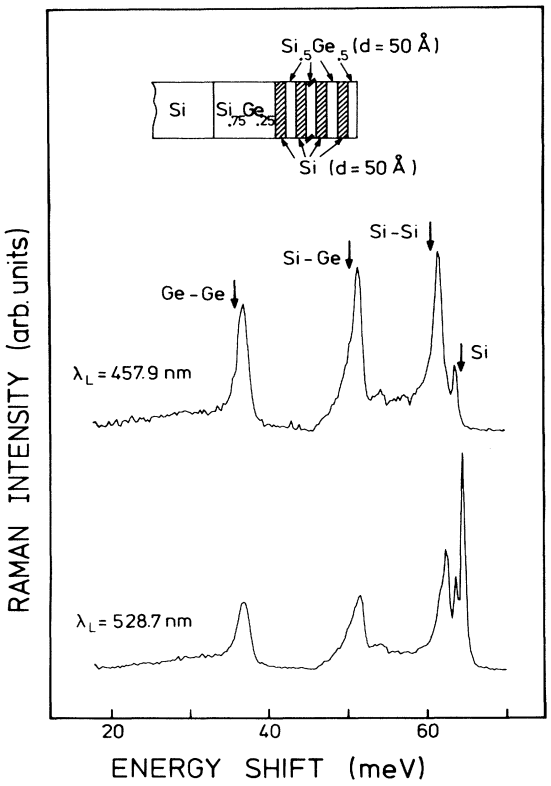

FIG. 1. Raman spectra of a $Si/Si_{0.5}Ge_{0.5}$ strained-layer superlattice. The information depth is varied by the use of two different laser lines. The arrows mark the energetic position of unstrained layers.

of Si and of $Si_{0.5}Ge_{0.5}$. Consequently, both types of layers are expected to be strained. The samples were grown by Si MBE on (100) Si substrates. Substrate preparation, growth procedure, and equipment are described elsewhere (see, e.g., Kasper[9] and Kasper and Wörner[10]). The growth temperature was 600 °C. Selective Sb doping was achieved by secondary implantation.[8] The concentration of doping atoms ranges from the low-10^{16}-cm^{-3} region to more than 10^{19} cm^{-3}. Sharp profiles are achieved. In our samples the position of Sb-doping spikes with respect to the Si/SiGe layer sequence was varied as described in Ref. 7.

In order to obtain direct information on built-in strains in the superlattice layers, we have studied the phonon frequencies by conventional Raman spectroscopy. The Raman spectrum of Si exhibits a single peak at $\hbar\omega = 64.5$ meV (520 cm^{-1}), which corresponds to the triply degenerate optical phonons of the Brillouin-zone center. In the presence of uniaxial strain the Raman peak splits into a doublet and a singlet and shifts linearly with strain as a consequence of the change of the elastic constants.[11] Only the singlet is observed in backscattering from (100) surfaces and lateral strain, which corresponds to a planar biaxial stress. Using the compliance constants and the phenomenological parameters for the strain-induced changes as determined by Chandrasekhar, Renucci, and Cardona,[12] we obtain the following relation between the frequency shift $\Delta\omega$ and the stress value: $\sigma = (2.49\ \text{kbar/cm}^{-1})\Delta\omega(\text{cm}^{-1})$. The biaxial stress is equivalent to the sum of a hydrostatic pressure and a uniaxial tension normal to the layers for layers under compression, and opposite for lateral tension. The situation is more complex for the Si_xGe_{1-x} alloy layers. The alloy spectrum shows three main peaks related to Ge-Ge, Si-Ge, and Si-Si vibrations. The frequencies of these modes depend on the composition of the alloy.[13,14] There is, however, little information on the strain dependence.[15] Recently, Cerdeira *et al.*[5] investigated several strained Si_xGe_{1-x} layers and found that the strain-induced shift of the Si-Ge vibration is linear with a slightly smaller slope than obtained for pure Si. It is suggested that this vibration is suitable for a quantitative evaluation of built-in strains.

In Fig. 1 we show two Raman spectra that are typical for our samples. Information of different layers is obtained by changing the laser line and consequently the penetration depth. With $\lambda_L = 457.9$ nm, the Raman spectrum exhibits only phonon lines from the superlattice. The expected positions for unstrained layers are marked by arrows. There is a clear upward shift of the three $Si_{0.5}Ge_{0.5}$ phonon lines. The optical mode originating from the Si layers, on the other hand, is shifted downwards. This indicates, as expected, a lateral compressive strain in the $Si_{0.5}Ge_{0.5}$ layers and a lateral tensile strain in Si. The spectrum obtained with $\lambda_L = 528.7$ nm exhibits two additional peaks, at 62 meV on top of the Si-Si vibrational mode of the strained $Si_{0.5}Ge_{0.5}$ alloy and at 64.5 meV, which corresponds to the phonon frequency of unstrained Si. These modes originate from the $Si_{0.75}Ge_{0.75}$ buffer layer and the Si substrate, which can be observed because of the large penetration depth of this laser line. The downward shift of the Si mode of the superlattice (7 cm^{-1} or 0.87 meV) corresponds to a strain of about 1%, which is equivalent to a stress value of 17 kbar (1.7 GPa). The shifts of the $Si_{0.5}Ge_{0.5}$ modes are found to be of the same size. This large strain causes a splitting of the different conduction-band valleys of about 150 meV, which has some consequence on the conduction-band ordering, as will be discussed later.

In Fig. 2 we show the temperature dependence of the Hall mobility for several samples as obtained with a standard van der Pauw method. In sample VS82 the Sb doping is incorporated in the center of the $Si_{0.5}Ge_{0.5}$ layers, in VS75 in the center of the Si layers, and in VS83 close to the interface, but still in the $Si_{0.5}Ge_{0.5}$ alloy layers. The decreasing mobility at low temperatures of sample VS75 is typical for highly doped *n*-type

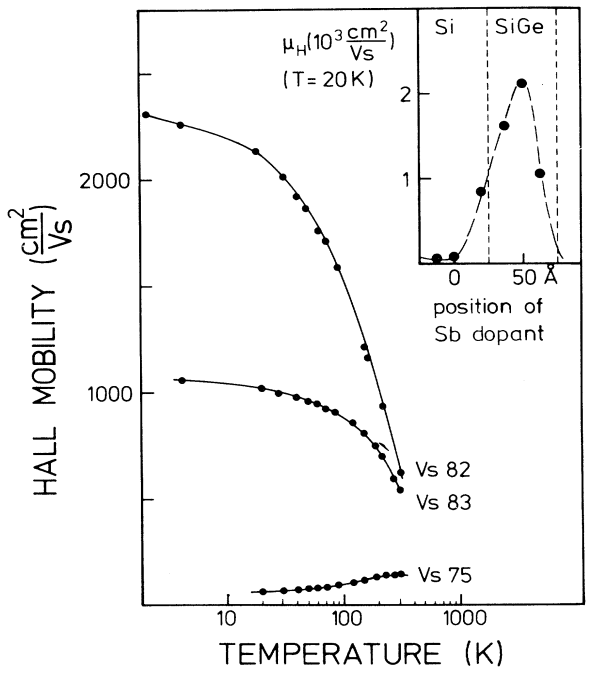

FIG. 2. Temperature dependence of the Hall mobility for samples with different doping positions in selectively doped $Si/Si_{0.5}Ge_{0.5}$ strained-layer superlattices. The doping positions are as follows: the center of the Si layers (VS75); in the $Si_{0.5}Ge_{0.5}$ layers, but close to the interface (VS83); and in the center of the $Si_{0.5}Ge_{0.5}$ layers (VS82). The inset shows the Hall mobility at $T = 20$ K vs doping position.

Si. In the other two samples the mobility is much improved at low temperatures. This is due to the effect of selective doping, where the ionized donors are separated in space from the carriers, resulting in a strong reduction of ionized impurity scattering.[16] The most surprising result, however, is the fact that one gets enhanced mobilities whenever the SB dopants are placed in the $Si_{0.5}Ge_{0.5}$ alloy layers, the material with the smaller band gap. This can be seen more clearly in the inset of Fig. 2, where the $T=20$ K Hall mobilities of six samples are plotted versus the position of the doping spike in the Si or $Si_{0.5}Ge_{0.5}$ layers. The mobility enhancement is strongly pronounced in the samples where the SiGe layers are doped. The small shift of the peak from the center of the layers of about 10 Å is caused by the doping method.[7]

Direct confirmation of the existence of a two-dimensional electron gas is obtained from measurements of Shubnikov–de Haas oscillations. Figure 3 shows the magnetoresistance of sample VS82 at $T=2$ K. The oscillation period observed with the magnetic field perpendicular to the layers leads to a two-dimensional electron density $n_s=(1.54\times10^{12})g_v$ cm^{-2}/layer; g_v is the valley degeneracy. With the assumption $g_v=2$, the resulting $n_s=3.08\times10^{12}$ cm^{-2} is in reasonable agreement with the total density obtained from Hall measurements, which gives $N_s\simeq4\times10^{13}$ cm^{-2} for the ten layers. No Shubnikov–de Haas oscillations are observed for B parallel to the layers. A similar behavior is found for the samples VS81 and VS83, the other two available samples with the doped region inside the SiGe layers. The total amplitude of the magnetoresistance oscillations is rather small (approximately 1% at 6 T). This is probably due to inhomogeneities of the carrier concentration from layer to layer. Slightly different carrier densities may also explain the weak anomaly observed around 4 T, where one peak is strongly damped as a result of a beating effect of closely spaced oscillation periods.

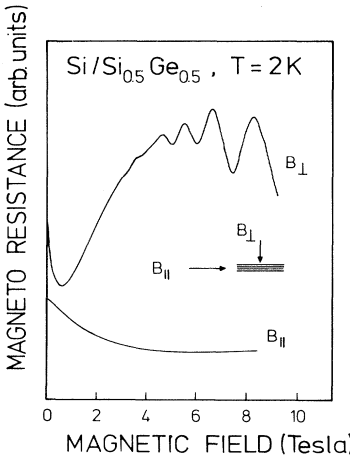

FIG. 3. Shubnikov–de Haas measurements at $T=2$ K for sample VS82. The lack of oscillations in parallel field confirms the two-dimensional character of the electron gas.

In order to determine the effective mass of the two-dimensional carrier systems, we also performed cyclotron-resonance experiments with a far-infrared laser that provides 890.7-GHz radiation. A broad cyclotron-resonance absorption line is observed which leads to an $\omega\tau$ between 2 and 3 and a cyclotron mass very close to $0.2m_0$, a value that is also observed in (100) Si inversion layers where only the twofold degenerate subbands are occupied.[17] This is further evidence that the electrons are situated in the Si layers rather than in the $Si_{0.5}Ge_{0.5}$ layers, as will be discussed in the next section.

From all these experimental data, we now construct a simple model of the band offsets and the potential wells in Si/Si_xGe_{1-x} strained-layer superlattices. The indirect gap of bulk Si_xGe_{1-x} has been investigated by Braunstein, Moore, and Herman.[18] For $Si_{0.5}Ge_{0.5}$, the band structure is very similar to that of Si. The conduction-band minima are found to be along the (100) directions close to the X point of the Brillouin zone. There is only little information on the band offsets for Si/Si_xGe_{1-x} heterojunctions. At $x=0.5$ the total band-gap difference is about 0.2 eV. There is some evidence that $\Delta E_v >> \Delta E_c$,[6] which leads to a band diagram as shown in Fig. 4(a). The strong uniaxial strain present in our superlattices, however, causes significant modifications. The effect of uniaxial stress on the conduction band has been studied for example by Balslev.[19] With applied stress along the (100) direc-

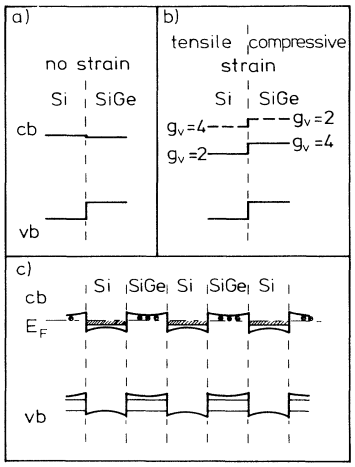

FIG. 4. Proposed band offsets at the interface of Si/Si_xGe_{1-x} heterojunctions: (a) in the absence of strain, (b) with lateral tensile strain in Si and lateral compressive strain in SiGe, and (c) real-space energy diagram of a strained-layer superlattice. The effect of strain on the valence band has been neglected.

tion, the sixfold degenerate conduction band is split into twofold and fourfold degenerate valleys. For uniaxial compression, two valleys are lowered in energy by 5.8 meV/kbar; the other four valleys are shifted upwards by 2.9 meV/kbar. For tensile strain along the (100) direction, the signs are reversed. The total splitting is 8.7 meV/kbar. Using the experimentally determined stress in our samples of about 17 kbar, we obtain a splitting of the conduction band of $\simeq 150$ meV.

The band diagram resulting from lateral stress in the layers is shown in Fig. 4(b). In-plane stress causes tensile strain in the Si layers and compressive strain in the SiGe layer, with opposite strains in the direction normal to the layer plane. The effect of strain on the valence band is not included in the figure. The strain-induced splittings and shifts of the conduction-band minima can easily lead to the situation that the conduction band of the wider-gap material Si is lower in energy than that of Si_xGe_{1-x}. For the strained-layer superlattice $Si/Si_{0.5}Ge_{0.5}$ with lateral tensile strain in the Si layers and lateral compressive strain in the $Si_{0.5}Ge_{0.5}$ layers, we propose the band diagram shown in Fig. 4(c). In *n*-type samples carrier confinement occurs in the Si layers. Up to high densities the carriers occupy the ground state of the twofold degenerate subband, which is favored by the type of strain, but also by the confinement in (100) direction.[20] The effect of electron mobility enhancement due to selective doping is therefore only achieved when the Si_xGe_{1-x} layers are doped. This is probably different when the type or size of strain is changed by use of other substrates or buffer layers.

In conclusion, we report on the first observation of two-dimensional electron systems in Si/Si_xGe_{1-x} strained-layer superlattices with enhanced low-temperature mobilities. From various experimental observations, a band model is proposed which leads to electron confinement in the Si layers. We want to emphasize that the built-in strain plays an important role in the ordering of the bands. This effect might also be significant in the actual values of band discontinuities of other heterostructures. The samples used for the present investigation are by no means optimized for maximum mobility. Improvements are probably achieved by increasing the space thickness, by lowering the carrier concentration, and last but not least, by lowering the background impurities. Such work is in progress.

The expert technical assistance of H. Kibble and K. H. Hieber is gratefully acknowledged. We thank E. Kasper encouraging SiGe work and for a critical reading of the manuscript.

[1]E. Kasper and H. J. Herzog, Appl. Phys. **8**, 199 (1975).

[2]J. C. Bean, T. T. Sheng, L. C. Feldman, A. T. Fiory, and R. T. Lynch, Appl. Phys. Lett. **44**, 102 (1984).

[3]J. C. Bean, L. C. Feldman, A. T. Fiory, S. Nakahara, and J. K. Robinson, J. Vac. Sci. Technol. A **2**, 436 (1984).

[4]E. Kasper and W. Papst, Thin Solid Films **37**, L5 (1976).

[5]F. Cerdeira, A. Pinczuk, J. C. Bean, B. Batlogg, and B. A. Wilson, Appl. Phys. Lett. **45**, 1138 (1984).

[6]R. People, J. C. Bean, D. V. Lang, A. M. Sergent, H. L. Störmer, K. W. Wecht, R. T. Lynch, and K. Baldwin, Appl. Phys. Lett. **45**, 1231 (1984).

[7]H. Jorke and H. J. Herzog, in Proceedings of the International Symposium on Si Molecular Beam Epitaxy, Toronto, Canada, 1985 (to be published).

[8]H. Jorke and H. Kibble, in Ref. 7.

[9]E. Kasper, Appl. Phys. A **28**, 129 (1982).

[10]E. Kasper and K. Wörner, in *Proceedings of the Second International Symposium on Very Large Scale Integration Science and Technology,* edited by K. E. Bean and G. A. Rozgonyi (Electrochemial Society, Pennington, 1984), p. 429.

[11]E. Anastassakis, A. Pinczuk, E. Burstein, F. H. Pollak, and M. Cardona, Solid State Commun. **8**, 133 (1970).

[12]M. Chandrasekhar, J. B. Renucci, M. Cardona, Phys. Rev. B **17**, 1623 (1978).

[13]M. A. Renucci, J. B. Renucci, and M. Cardona, in *Proceedings of the Second International Conference on Light Scattering in Solids,* edited by M. Balkanski (Flammarion, Paris, 1971), p. 326.

[14]J. S. Lannin, Phys. Rev. B **16**, 1510 (1977).

[15]J. B. Renucci, M. A. Renucci, and M. Cardona, Solid State Commun. **9**, 1651 (1971).

[16]H. L. Störmer, R. Dingle, A. C. Gossard, W. Wiegmann, and M. D. Sturge, Solid State Commun. **29**, 705 (1979).

[17]G. Abstreiter, J. P. Kotthaus, J. F. Koch, and G. Dorda, Phys. Rev. B **14**, 2480 (1976).

[18]R. Braunstein, A. R. Moore, and F. Herman, Phys. Rev. **109**, 695 (1958).

[19]J. Balslev, Phys. Rev. **143**, 636 (1966).

[20]T. Ando, A. B. Fowler, and F. Stern, Rev. Mod. Phys. **54**, 437 (1982).